

Arbitrary high-order structure-preserving schemes for the generalized Rosenau-type equation

Chaolong Jiang^{1,2}, Xu Qian^{2*}, Songhe Song², and Chenxuan Zheng¹

¹ Yunnan Key Laboratory of Applied Mathematics, School of Statistics and Mathematics, Yunnan University of Finance and Economics, Kunming 650221, P.R. China

² Department of Mathematics, College of Liberal Arts and Science, National University of Defense Technology, Changsha, 410073, P.R. China

Abstract

In this paper, we are concerned with arbitrarily high-order momentum-preserving and energy-preserving schemes for solving the generalized Rosenau-type equation, respectively. The derivation of the momentum-preserving schemes is made within the symplectic Runge-Kutta method, coupled with the standard Fourier pseudo-spectral method in space. Unlike the momentum-preserving scheme, the energy-preserving one relies on the use of the quadratic auxiliary variable approach and the symplectic Runge-Kutta method, as well as the standard Fourier pseudo-spectral method. Extensive numerical tests and comparisons are also addressed to illustrate the performance of the proposed schemes.

AMS subject classification: 65M06, 65M70

Keywords: Momentum-preserving, energy-preserving, high-order, symplectic Runge-Kutta method, Rosenau equation.

1 Introduction

To overcome the shortcomings of the Korteweg-de Vries (KdV) equation, the Rosenau equation is proposed to describe the dynamics of dense discrete systems[23]. Subsequently, some viscous terms are added to the Rosenau equation for the further consideration of nonlinear waves. In this paper, we consider the following generalized Rosenau-type equation

$$\begin{cases} \partial_t u(x, t) + \kappa \partial_x u(x, t) - \delta \partial_{xxt} u(x, t) + b \partial_{xxx} u(x, t) \\ \quad + \alpha \partial_{xxxxt} u(x, t) + \beta \partial_x (u(x, t)^p), \quad x \in \Omega \subset \mathbb{R}, \quad t > 0, \\ u(x, 0) = u_0(x), \quad x \in \Omega \subset \mathbb{R}, \end{cases} \quad (1.1)$$

where t is the time variable, x is the spatial variable, $u := u(x, t)$ is the real-valued wave function, $\kappa, \delta > 0, b, \alpha > 0$ and β are given real constants, $u_0(x)$ is a given initial condition, $\Omega = [x_l, x_r]$ is a bounded domain, and the periodic boundary condition is imposed on $\partial\Omega$.

When u is assumed to be smooth, the equation (1.1) satisfies the following Hamiltonian formulation

$$u_t = \mathcal{J} \frac{\delta \mathcal{H}}{\delta u}, \quad (1.2)$$

*Correspondence author. Email: qianxu@nudt.edu.cn.

where $\mathcal{J} = -(1 - \delta\partial_{xx} + \alpha\partial_{xxxx})^{-1}\partial_x$ is a Hamiltonian operator and \mathcal{H} is the Hamiltonian functional, namely

$$\mathcal{H}(t) = \int_{\Omega} \left(\frac{\kappa}{2}u^2 - \frac{b}{2}u_x^2 + \frac{\beta}{p+1}u^{p+1} \right) dx, \quad t \geq 0, \quad (1.3)$$

Besides the Hamiltonian energy (1.3), the equation (1.1) also conserves the mass

$$\mathcal{M}(t) = \int_{\Omega} u dx \equiv \mathcal{M}(0), \quad t \geq 0, \quad (1.4)$$

and momentum

$$\mathcal{I}(t) = \int_{\Omega} \left(\frac{1}{2}u^2 + \frac{\delta}{2}u_x^2 + \frac{\alpha}{2}u_{xx}^2 \right) dx \equiv \mathcal{I}(0), \quad t \geq 0. \quad (1.5)$$

In the numerical computation of such Hamiltonian partial differential equations, it is often preferable to design some special numerical schemes that inherit one or more intrinsic properties of the original system exactly in a discrete sense; they are called structure-preserving schemes. In [5], Chung proposed an implicit finite difference (IFD) scheme, which can satisfy the discrete analogue of momentum (1.5). Furthermore, they prove rigorously in mathematics that the scheme is second-order accurate in time and space. Subsequently, Omrani et al.[19] developed a linearly implicit momentum-preserving finite difference scheme for the classical Rosenau equation, in which a linear system is to be solved at every time step. Thus it is computationally much cheaper than that of the IFD scheme. Over the years, various momentum-preserving schemes for the equation (1.1) have been proposed and analyzed (e.g., see Refs [1, 2, 12, 18, 20, 27, 28, 29, 30, 31]). However, to the best of our knowledge, all of existing momentum-preserving schemes are only second-order accurate in time at most. It has been shown in [10, 16] that, compared with the second-order accurate schemes, the high-order accurate ones not only provide smaller numerical errors as a large time step chosen, but also will be more advantages in the robustness. Consequently, the first aim of this paper is to present a novel paradigm for developing arbitrary high-order momentum-preserving schemes for the equation (1.1).

Besides the momentum conservation law (1.5), the equation (1.1) also satisfies the Hamiltonian energy (1.3), which is one of the most important first integrals of the Hamiltonian system. Based on the averaged vector field method [21], Cai et al. [3] proposed a second-order energy-preserving scheme, and two fourth-order energy-preserving schemes are then proposed by using the composition ideas [11]. Nevertheless, it is shown in [11] that the high-order schemes obtained by the composition method will be at the price of a terrible zig-zag of the step points (see Fig. 4.2 in Ref. [11]), which may be tedious and time consuming. Thus, the construction of high-order energy-preserving schemes for the Rosenau equation (1.1) seems to be still at its beginning stage. In this paper, the second aim is to present a new strategy for proposing arbitrary high-order energy-preserving schemes for the Rosenau equation (1.1), which is inspired by the idea of the quadratic auxiliary variable (QAV) approach[9].

The rest of this paper is organized as follows. In Section 2, the high-order momentum-preserving and energy-preserving schemes for the equation (1.1) are proposed, respectively and their structure-preserving properties are proved in details. Extensive numerical examples and some comparisons are addressed to illustrate the performance of the proposed schemes in Section 4. We draw some conclusions in Section 5.

2 High-order structure-preserving schemes

In this section, we will propose a novel class of high-order momentum-preserving schemes and energy-preserving schemes for the equation (1.1), respectively.

To be the start, let the mesh sizes $h = \frac{x_r - x_l}{N}$ with an even positive integer N , and denote the grid points by $x_j = jh$ for $j = 0, 1, 2, \dots, N$; set u_j be the numerical approximation of $u(x_j, t)$ for $j = 0, 1, \dots, N$, and $U := (u_0, u_1, \dots, u_{N-1})^T$ be the solution vector; we also define the discrete inner product, l^2 -norm and l^∞ -norm as, respectively,

$$\langle U, V \rangle_h = h \sum_{j=0}^{N-1} u_j v_j, \quad \|U\|_h^2 = \langle U, U \rangle_h, \quad \|U\|_{h, \infty} = \max_{0 \leq j < N-1} |u_j|.$$

In addition, we denote ‘ \cdot ’ as the element product of vectors U and V , that is

$$U \cdot V = (u_0 v_0, u_1 v_1, \dots, u_{N-1} v_{N-1})^T.$$

For brevity, we denote $U \cdot U$ as U^2 .

As achieving high order accuracy in time, the spatial accuracy shall be comparable to that of the time-discrete discretization. Actually, we consider the periodic boundary condition in this paper, so that the Fourier pseudo-spectral method is a very good choice because of the high order accuracy and the fast Fourier transform (FFT) algorithm. Thus, we first expounded the Fourier pseudo-spectral method, as follows.

Let the interpolation space as

$$\mathcal{S}_h = \text{span}\{l_j(x), 0 \leq j \leq N-1\}$$

where $l_j(x)$ is trigonometric polynomials of degree $N/2$ given by

$$l_j(x) = \frac{1}{N} \sum_{k=-N/2}^{N/2} \frac{1}{a_k} e^{ik\mu(x-x_j)},$$

with $a_k = \begin{cases} 1, & |k| < \frac{N}{2}, \\ 2, & |k| = \frac{N}{2}, \end{cases}$ $\mu = \frac{2\pi}{x_r - x_l}$. We then define the interpolation operator $P_N : C(\Omega) \rightarrow \mathcal{S}_h$ as:

$$P_N u(x, t) = \sum_{k=0}^{N-1} u_k(t) l_k(x),$$

where $u_k(t) = u(x_k, t)$, $k = 0, 1, 2, \dots, N-1$.

Taking the partial derivative with respect to x at the collocation points x_j , we have

$$\frac{\partial^r P_N u(x_j, t)}{\partial x^r} = \sum_{k=0}^{N-1} u_k(t) \frac{d^r l_k(x_j)}{dx^r} = \sum_{k=0}^{N-1} (D_r)_{j,k} u_k(t), \quad j = 0, 1, \dots, N-1, \quad (2.1)$$

where D_r represents the spectral differential matrix with elements given by

$$(D_r)_{j,k} = \frac{d^r l_k(x_j)}{dx^r}, \quad j, k = 0, 1, \dots, N-1.$$

In particular, we have[14, 26]

$$(D_1)_{j,k} = \begin{cases} \frac{1}{2} \mu (-1)^{j+k} \cot(\mu \frac{x_j - x_k}{2}), & j \neq k, \\ 0, & j = k, \end{cases}$$

$$(D_2)_{j,k} = \begin{cases} \frac{1}{2}\mu^2(-1)^{j+k+1} \csc^2(\mu\frac{x_j - x_k}{2}), & j \neq k, \\ -\mu^2\frac{N^2 + 2}{12}, & j = k, \end{cases}$$

$$(D_3)_{j,k} = \begin{cases} \frac{3\mu^3}{4}(-1)^{j+k} \cos(\mu\frac{x_j - x_k}{2}) \csc^3(\mu\frac{x_j - x_k}{2}) \\ \quad + \frac{\mu^3 N^2}{8}(-1)^{j+k+1} \cot(\mu\frac{x_j - x_k}{2}), & j \neq k, \\ 0, & j = k, \end{cases}$$

and

$$(D_4)_{j,k} = \begin{cases} \mu^4(-1)^{j+k} \csc^2(\mu\frac{x_j - x_k}{2}) \left(\frac{N^2}{4} - \frac{1}{2} - \frac{3}{2} \cot^2(\mu\frac{x_j - x_k}{2}) \right), & j \neq k, \\ \mu^4 \left(\frac{N^4}{80} + \frac{N^2}{12} - \frac{1}{30} \right), & j = k. \end{cases}$$

Remark 2.1. We should note that [8]

$$D_r = \begin{cases} \mathcal{F}_N^H \Lambda^r \mathcal{F}_N, & r \text{ is an odd integer,} \\ \mathcal{F}_N^H \tilde{\Lambda}^r \mathcal{F}_N, & r \text{ is an even integer,} \end{cases}$$

where Λ and $\tilde{\Lambda}$ are

$$\Lambda = \text{diag}\left(i\mu\left[0, 1, \dots, \frac{N}{2} - 1, 0, -\frac{N}{2} + 1, \dots, -2, -1\right]\right),$$

$$\tilde{\Lambda} = \text{diag}\left(i\mu\left[0, 1, \dots, \frac{N}{2} - 1, \frac{N}{2}, -\frac{N}{2} + 1, \dots, -2, -1\right]\right),$$

and \mathcal{F}_N is the discrete Fourier transform (DFT) and \mathcal{F}_N^H represents the conjugate transpose of \mathcal{F}_N .

We set $t_n = n\tau$, and $t_{ni} = t_n + c_i\tau$, $i = 1, 2, \dots, s$, $n = 0, 1, 2, \dots$, where τ is the time step and c_1, c_2, \dots, c_s are distinct real numerbers (usually $0 \leq c_i \leq 1$). The approximations of the function $u(x, t)$ at points (x_j, t_n) and (x_j, t_{ni}) are denoted by u_j^n and u_j^{ni} , respectively.

2.1 High-order momentum-preserving scheme

In this section, we propose a class of high-order momentum-preserving schemes for the equation (1.1). To be the start, we rewrite (1.1) into

$$\mathcal{A}u_t = \mathcal{F}(u)u, \quad \mathcal{F}(u) = -\left[\kappa\partial_x + b\partial_{xxx} + \frac{p\beta}{p+1}(u^{p-1}\partial_x + \partial_x(u^{p-1}))\right], \quad (2.2)$$

where $\mathcal{A} = 1 - \delta\partial_{xx} + \alpha\partial_{xxxx}$ is a self-adjoint operator, $\mathcal{F}(u)$ is an anti-adjoint operator and $\mathcal{F}(u)u$ is defined by

$$\mathcal{F}(u)u = -\left[\kappa\partial_x u + b\partial_{xxx} u + \frac{p\beta}{p+1}(u^{p-1}\partial_x u + \partial_x(u^p))\right].$$

The Fourier pseudo-spectral method presented as above is then applied to solve (2.2) in space and we obtain

$$\mathcal{A}_h \frac{d}{dt} U = \mathcal{F}_h(U)U, \quad \mathcal{F}_h(U) = -\left[\kappa D_1 + b D_3 + \frac{p\beta}{p+1}(U^{p-1} D_1 + D_1(U^{p-1}))\right], \quad (2.3)$$

where $\mathcal{A}_h = I - \delta D_2 + \alpha D_4$ is a symmetric matrix, $\mathcal{F}_h(U)$ is anti-symmetric for U , and $\mathcal{F}_h(U)U$ is defined by

$$\mathcal{F}_h(U)U = -\left[\kappa D_1 U + b D_3 U + \frac{p\beta}{p+1}(U^{p-1} \cdot D_1 U + D_1(U^p))\right]. \quad (2.4)$$

Theorem 2.1. *The semi-discrete system (2.3) preserves the following semi-discrete momentum conservation law*

$$\frac{d}{dt} I_h(t) = 0, \quad I_h(t) = \frac{1}{2} \langle \mathcal{A}_h U, U \rangle_h, \quad t \geq 0. \quad (2.5)$$

Proof. *With noting the anti-symmetric property of $\mathcal{F}_h(U)$ for U , we have*

$$\frac{d}{dt} I_h(t) = \langle \mathcal{A}_h \frac{d}{dt} U, U \rangle_h = \langle \mathcal{F}_h(U)U, U \rangle_h = 0,$$

which completes the proof. □

Theorem 2.2. *If $p = 2$, the semi-discrete system (2.3) preserves the following semi-discrete mass*

$$\frac{d}{dt} M_h(t) = 0, \quad M_h(t) = \langle U, \mathbf{1} \rangle_h, \quad t \geq 0. \quad (2.6)$$

Proof. *It follows from (2.3) that*

$$\frac{d}{dt} M_h(t) = \langle \mathcal{A}_h^{-1} \mathcal{F}_h(U)U, \mathbf{1} \rangle_h = \langle \mathcal{F}_h(U)U, \mathcal{A}_h^{-1} \mathbf{1} \rangle_h = \langle \mathcal{F}_h(U)U, \mathbf{1} \rangle_h. \quad (2.7)$$

With (2.4), we have

$$\begin{aligned} \langle \mathcal{F}_h(U)U, \mathbf{1} \rangle_h &= -\langle \kappa D_1 U + b D_3 U + \frac{\beta}{p+1}(U^{p-1} \cdot D_1 U + D_1(U^p)), \mathbf{1} \rangle_h \\ &= -\frac{p\beta}{p+1} \langle D_1 U, U^{p-1} \rangle_h. \end{aligned} \quad (2.8)$$

As $p = 2$, we obtain from the above equation

$$\langle \mathcal{F}_h(U)U, \mathbf{1} \rangle_h = 0,$$

which implies that

$$\frac{d}{dt} M_h(t) = 0.$$

This completes the proof. □

Remark 2.2. *The Fourier spectral differential matrix D_1 cannot satisfy the discrete equation*

$$\langle D_1 U^p, \mathbf{1} \rangle_h = p \langle D_1 U, U^{p-1} \rangle_h. \quad (2.9)$$

Thus, the system (2.3) cannot conserve semi-discrete mass (2.6), as $p > 2$.

We then apply an RK method to the system (2.3) in time to give a class of fully discrete schemes for the equation (1.1), as follows:

Scheme 2.1. Let $b_i, a_{ij}(i, j = 1, \dots, s)$ be real numbers and let $c_i = \sum_{j=1}^s a_{ij}$. For the given U^n , an s -stage Runge-Kutta method is given by

$$\begin{cases} \mathcal{A}_h K_i^n = \mathcal{F}_h(U^{ni})U^{ni}, & U^{ni} = U^n + \tau \sum_{j=1}^s a_{ij} K_j^n, \quad i = 1, 2, \dots, s, \\ U^{n+1} = U^n + \tau \sum_{i=1}^s b_i K_i^n. \end{cases} \quad (2.10)$$

Theorem 2.3. If the coefficients of the RK method satisfy

$$b_i a_{ij} + b_j a_{ji} = b_i b_j, \quad \forall i, j = 1, \dots, s, \quad (2.11)$$

Scheme 2.1 conserves the following discrete momentum

$$I_h^{n+1} = I_h^n, \quad I_h^n = \frac{1}{2} \langle U^n, \mathcal{A}_h U^n \rangle_h, \quad n = 0, 1, 2, \dots. \quad (2.12)$$

Proof. It follows from the second equality of (2.10) that

$$\begin{aligned} I_h^{n+1} - I_h^n &= \frac{1}{2} \langle U^{n+1}, \mathcal{A}_h U^{n+1} \rangle_h - \frac{1}{2} \langle U^n, \mathcal{A}_h U^n \rangle_h \\ &= \frac{1}{2} \langle U^n + \tau \sum_{i=1}^s b_i K_i^n, \mathcal{A}_h (U^n + \tau \sum_{j=1}^s b_j K_j^n) \rangle_h - \frac{1}{2} \langle U^n, \mathcal{A}_h U^n \rangle_h \\ &= \frac{\tau}{2} \sum_{i=1}^s b_i \langle U^n, \mathcal{A}_h K_i^n \rangle_h + \frac{\tau}{2} \sum_{i=1}^s b_i \langle K_i^n, \mathcal{A}_h U^n \rangle_h + \frac{\tau^2}{2} \sum_{i,j=1}^s b_i b_j \langle K_i^n, \mathcal{A}_h K_j^n \rangle_h. \end{aligned} \quad (2.13)$$

With noting

$$\begin{aligned} \frac{\tau}{2} \sum_{i=1}^s b_i \langle U^n, \mathcal{A}_h K_i^n \rangle_h &= \frac{\tau}{2} \sum_{i=1}^s b_i \langle U^{ni} - \tau \sum_{j=1}^s a_{ij} K_j^n, \mathcal{A}_h K_i^n \rangle_h \\ &= \frac{\tau}{2} \sum_{i=1}^s b_i \langle U^{ni}, \mathcal{A}_h K_i^n \rangle_h - \frac{\tau^2}{2} \sum_{i,j=1}^s b_j a_{ji} \langle K_i^n, \mathcal{A}_h K_j^n \rangle_h. \end{aligned} \quad (2.14)$$

Similarly, we have

$$\frac{\tau}{2} \sum_{i=1}^s b_i \langle K_i^n, \mathcal{A}_h U^n \rangle_h = \frac{\tau}{2} \sum_{i=1}^s b_i \langle K_i^n, \mathcal{A}_h U^{ni} \rangle_h - \frac{\tau^2}{2} \sum_{i,j=1}^s b_i a_{ij} \langle K_i^n, \mathcal{A}_h K_j^n \rangle_h. \quad (2.15)$$

We insert (2.14) and (2.15) into (2.13) and then use the symmetry of \mathcal{A}_h to obtain

$$\begin{aligned} I_h^{n+1} - I_h^n &= \frac{\tau}{2} \sum_{i=1}^s b_i [\langle U^{ni}, \mathcal{A}_h K_i^n \rangle_h + \langle K_i^n, \mathcal{A}_h U^{ni} \rangle_h] \\ &\quad + \frac{\tau^2}{2} \sum_{i,j=1}^s (b_i b_j - b_i a_{ij} - b_j a_{ji}) \langle K_i^n, \mathcal{A}_h K_j^n \rangle_h \\ &= \tau \sum_{i=1}^s b_i \langle U^{ni}, \mathcal{A}_h K_i^n \rangle_h + \frac{\tau^2}{2} \sum_{i,j=1}^s (b_i b_j - b_i a_{ij} - b_j a_{ji}) \langle K_i^n, \mathcal{A}_h K_j^n \rangle_h. \end{aligned}$$

The condition (2.11) together with the equality

$$\langle U^{ni}, \mathcal{A}_h K_i^n \rangle_h = \langle U^{ni}, \mathcal{F}_h(U^{ni})U^{ni} \rangle_h = 0$$

implies $I_h^{n+1} = I_h^n$. This completes the proof. \square

Theorem 2.4. As $p = 2$, **Scheme 2.1** conserves the discrete mass, as follows:

$$M_h^{n+1} = M_h^n, \quad M_h^n = \langle U^n, \mathbf{1} \rangle_h, \quad n = 0, 1, 2, \dots \quad (2.16)$$

Proof. It follows from (2.10) that

$$\begin{aligned} M_h^{n+1} - M_h^n &= \tau \sum_{i=1}^s b_i \langle K_i^n, \mathbf{1} \rangle_h \\ &= \tau \sum_{i=1}^s b_i \langle \mathcal{A}_h^{-1} \mathcal{F}_h(U^{ni}) U^{ni}, \mathbf{1} \rangle_h \\ &= \tau \sum_{i=1}^s b_i \langle \mathcal{F}_h(U^{ni}) U^{ni}, \mathbf{1} \rangle_h \\ &= -\tau \sum_{i=1}^s b_i \langle \kappa D_1 U^{ni} + b D_3 U^{ni} + \frac{p\beta}{p+1} ((U^{ni})^{p-1} \cdot D_1 U^{ni} + D_1((U^{ni})^p)), \mathbf{1} \rangle_h \\ &= -\frac{p\beta}{p+1} \langle D_1 U^{ni}, (U^{ni})^{p-1} \rangle_h. \end{aligned}$$

Combining $p = 2$ and the antisymmetry of D_1 , we have

$$\langle D_1 U^{ni}, (U^{ni})^{p-1} \rangle_h = 0,$$

which implies (2.16). This completes the proof. \square

Remark 2.3. Assume that the initial condition $u_0(x)$ is sufficiently smooth, then it follows from (2.16) that the numerical solution of **Scheme 2.1** satisfies

$$\begin{aligned} &\sqrt{\|U^n\|_h^2 + \delta \langle -D_2 U^n, U^n \rangle_h + \alpha \langle D_4 U^n, U^n \rangle_h} \\ &= \sqrt{\|U^0\|_h^2 + \delta \langle -D_2 U^0, U^0 \rangle_h + \alpha \langle D_4 U^0, U^0 \rangle_h} \leq C, \end{aligned}$$

which implies that

$$\|U^n\|_h \leq C, \quad \langle -D_2 U^n, U^n \rangle_h \leq C, \quad \langle D_4 U^n, U^n \rangle_h \leq C,$$

is uniformly bounded. Thus, **Scheme 2.1** is unconditionally stable.

Remark 2.4. If we take c_1, c_2, \dots, c_s as the zeros of the s th shifted Legendre polynomial

$$\frac{d^s}{dx^s} (x^s (x-1)^s),$$

the RK (or collocation) method based on these nodes has the order $2s$ and satisfies the condition (2.11) (see Refs. [11, 24, 25] and references therein). The RK coefficients for $s = 2$ and $s = 3$ (denoted by 4th-Gauss method and 6th-Gauss method, respectively) are given in Table 1 (e.g., see Ref. [11]). In addition, we introduce two notations, as follows:

- 4th-MPS: using 4th-Gauss collocation method to **Scheme 2.1**;
- 6th-MPS: using 6th-Gauss collocation method to **Scheme 2.1**.

$$\begin{array}{c}
c \mid A \\
\hline
b^T
\end{array}
=
\begin{array}{c|cc}
\frac{1}{2} - \frac{\sqrt{3}}{6} & \frac{1}{4} & \frac{1}{4} - \frac{\sqrt{3}}{6} \\
\frac{1}{2} + \frac{\sqrt{3}}{6} & \frac{1}{4} + \frac{\sqrt{3}}{6} & \frac{1}{4} \\
\hline
& \frac{1}{2} & \frac{1}{2}
\end{array}$$

$$\begin{array}{c}
c \mid A \\
\hline
b^T
\end{array}
=
\begin{array}{c|ccc}
\frac{1}{2} - \frac{\sqrt{15}}{10} & \frac{5}{36} & \frac{2}{9} - \frac{\sqrt{15}}{15} & \frac{5}{36} - \frac{\sqrt{15}}{30} \\
\frac{1}{2} & \frac{5}{36} + \frac{\sqrt{15}}{24} & \frac{2}{9} & \frac{5}{36} - \frac{\sqrt{15}}{24} \\
\frac{1}{2} + \frac{\sqrt{15}}{10} & \frac{5}{36} + \frac{\sqrt{15}}{30} & \frac{2}{9} + \frac{\sqrt{15}}{15} & \frac{5}{36} \\
\hline
& \frac{5}{18} & \frac{4}{9} & \frac{5}{18}
\end{array}$$

Table 1: Gauss methods of order 4 and 6.

2.2 High-order energy-preserving scheme

In this section, we propose a class of high-order energy-preserving schemes for the equation (1.1). Inspired by [9, 17], we first shall introduce appropriate quadratic auxiliary variables to reformulate the Hamiltonian energy into a quadratic form. For clarity, we take $p = 2, 3$ and 5 as examples to expound this procedure, as follows:

Case I: when $p = 2$, we set

$$q := q(x, t) = u^2. \quad (2.17)$$

Then, the Hamiltonian energy (1.3) is rewritten into

$$\mathcal{H}(t) = \int_{\Omega} \left(\frac{\kappa}{2} u^2 - \frac{b}{2} u_x^2 + \frac{\beta}{3} uq \right) dx, \quad t \geq 0, \quad (2.18)$$

and according to the energy variational principle, we obtain the following reformulated system from (1.2)

$$\begin{cases} \partial_t u = \mathcal{J} \left(\kappa u + b u_{xx} + \frac{\beta}{3} q + \frac{2\beta}{3} u^2 \right), \\ \partial_t q = 2u \cdot \partial_t u, \end{cases} \quad (2.19)$$

with the consistent initial conditions

$$u(x, 0) = u_0(x), \quad q(x, 0) = (u_0(x))^2. \quad (2.20)$$

Case II: for $p = 3$, the quadratic auxiliary variable is introduced as (2.17), and the quadratic energy is given by

$$\mathcal{H}(t) = \int_{\Omega} \left(\frac{\kappa}{2} u^2 - \frac{b}{2} u_x^2 + \frac{\beta}{4} q^2 \right) dx, \quad t \geq 0, \quad (2.21)$$

which implies that the reformulated system is given by

$$\begin{cases} \partial_t u = \mathcal{J} \left(\kappa u + b u_{xx} + \beta uq \right), \\ \partial_t q = 2u \cdot \partial_t u, \end{cases} \quad (2.22)$$

with the consistent initial conditions (2.20).

Case III: As $p = 5$, we start with introducing auxiliary variables

$$q_1 := q_1(x, t) = u^2, \quad q_2 := q_2(x, t) = uq_1, \quad (2.23)$$

and then rewrite the Hamiltonian energy (1.3) as

$$\mathcal{H}(t) = \int_{\Omega} \left(\frac{\kappa}{2} u^2 - \frac{b}{2} u_x^2 + \frac{\beta}{6} q_2^2 \right) dx, \quad t \geq 0. \quad (2.24)$$

Similarly, we obtain reformulated system from (1.2), as follows:

$$\begin{cases} \partial_t u = \mathcal{J} \left(\kappa u + b u_{xx} + \frac{\beta}{3} q_2 (q_1 + 2u^2) \right), \\ \partial_t q_1 = 2u \cdot \partial_t u, \\ \partial_t q_2 = \partial_t u \cdot q_1 + u \cdot \partial_t q_1 = \partial_t u \cdot q_1 + 2u^2 \cdot \partial_t u, \end{cases} \quad (2.25)$$

with the consistent initial conditions

$$u(x, 0) = u_0(x), \quad q_1(x, 0) = (u_0(x))^2, \quad q_2(x, 0) = u_0(x, 0) q_1(x, 0). \quad (2.26)$$

For simplicity, in the following construction of the energy-preserving schemes, we consider the parameter $p = 2$ for the equation (1.1). Note that the extensions to the parameter $p > 2$ are straightforward.

Theorem 2.5. *Under the periodic boundary condition, the reformulated system (2.19) conserves the mass (1.4).*

Proof. *It follows from the first equation of (2.19), together with the periodic boundary condition that*

$$\begin{aligned} \frac{d}{dt} \mathcal{M}(t) &= (\partial_t u, 1) \\ &= \left(\mathcal{J} \left(\kappa u + b u_{xx} + \frac{\beta}{3} q + \frac{2\beta}{3} u^2 \right), 1 \right) \\ &= - \left(\partial_x \left(\kappa u + b u_{xx} + \frac{\beta}{3} q + \frac{2\beta}{3} u^2 \right), (1 - \delta_{xx} + \alpha \partial_{xxx})^{-1} \mathbf{1} \right) \\ &= - \left(\partial_x \left(\kappa u + b u_{xx} + \frac{\beta}{3} q + \frac{2\beta}{3} u^2 \right), 1 \right) \\ &= 0. \end{aligned}$$

This completes the proof. □

Theorem 2.6. *Under the periodic boundary condition, the reformulation (2.19) preserves the following invariants*

$$\mathcal{H}_{1,1} = q - u^2 = 0, \quad (2.27)$$

$$\mathcal{H}(t) = \int_{\Omega} \left(\frac{\kappa}{2} u^2 - \frac{b}{2} u_x^2 + \frac{\beta}{3} u q \right) dx, \quad t \geq 0. \quad (2.28)$$

Proof. *It follows from the second equation of (2.19) that*

$$\partial_t \mathcal{H}_{1,1} = \partial_t q - 2u \cdot \partial_t u = 0. \quad (2.29)$$

According to (2.17) and (2.19) together with the anti-adjoint property of \mathcal{J} , we have

$$\begin{aligned} \frac{d}{dt} \mathcal{H}(t) &= \int_{\Omega} \left(\kappa u \partial_t u - b \partial_x u \partial_{xt} u + \frac{\beta}{3} (q \partial_t u + u \partial_t q) \right) dx \\ &= \int_{\Omega} \left(\kappa u \partial_t u + b \partial_{xx} u \partial_t u + \frac{\beta}{3} (q + 2u^2) \partial_t u \right) dx \\ &= \int_{\Omega} \left(\kappa u + b \partial_{xx} u + \frac{\beta}{3} (q + 2u^2) \right) \mathcal{J} \left(\kappa u + b u_{xx} + \frac{\beta}{3} (q + 2u^2) \right) dx \\ &= 0. \end{aligned}$$

This completes the proof. □

Next, we apply an RK method to the system (2.19) in time, together with the Fourier pseudo-spectral method in space to give a class of fully discrete schemes for (2.19), as follows:

Scheme 2.2. Let b_i, a_{ij} ($i, j = 1, \dots, s$) be real numbers and let $c_i = \sum_{j=1}^s a_{ij}$. For the given (U^n, Q^n) , an s -stage Runge-Kutta method is given by

$$\begin{cases} K_i^n = \mathcal{J}_h \left(\kappa U^{ni} + b D_2 U^{ni} + \frac{\beta}{3} (Q^{ni} + 2(U^{ni})^2) \right), \\ U^{ni} = U^n + \tau \sum_{j=1}^s a_{ij} K_j^n, \quad \mathcal{J}_h = -(I - \delta D_2 + \alpha D_4)^{-1} D_1, \\ Q^{ni} = Q^n + \tau \sum_{j=1}^s a_{ij} L_j^n, \quad L_i^n = 2U^{ni} \cdot K_i^n, \quad i = 1, 2, \dots, s, \end{cases} \quad (2.30)$$

and (U^{n+1}, Q^{n+1}) is then updated by

$$U^{n+1} = U^n + \tau \sum_{i=1}^s b_i K_i^n, \quad Q^{n+1} = Q^n + \tau \sum_{i=1}^s b_i L_i^n. \quad (2.31)$$

Theorem 2.7. If the coefficients of (2.30) and (2.31) satisfy (2.11), **Scheme 2.2** preserves the following discrete invariants

$$H_{1,1}^{n+1} = H_{1,1}^n, \quad H_{1,1}^n = Q^n - (U^n)^2, \quad (2.32)$$

$$\mathcal{E}_h^{n+1} = \mathcal{E}_h^n, \quad \mathcal{E}_h^n = \frac{\kappa}{2} \|U^n\|^2 + \frac{b}{2} \langle D_2 U^n, U^n \rangle_h + \frac{\beta}{3} \langle U^n, Q^n \rangle_h, \quad n = 0, 1, \dots, \dots \quad (2.33)$$

Proof. It follows from (2.31) that

$$\begin{aligned} H_{1,1}^{n+1} - H_{1,1}^n &= Q^{n+1} - Q^n - (U^{n+1})^2 + (U^n)^2 \\ &= \tau \sum_{j=1}^s b_j L_j^n - \tau \sum_{i=1}^s b_i K_i^n \cdot U^n - \tau \sum_{i=1}^s b_i U^n \cdot K_i^n - \tau^2 \sum_{i,j=1}^s b_i b_j K_i^n \cdot K_j^n. \end{aligned}$$

Using the equality $U^n = U^{ni} - \tau \sum_{j=1}^s a_{ij} K_j^n$ and $L_i^n = 2U^{ni} \cdot K_i^n$, together with (2.11), we can obtain from the above equation

$$\begin{aligned} H_{1,1}^{n+1} - H_{1,1}^n &= \tau \sum_{j=1}^s b_j L_j^n - 2\tau \sum_{i=1}^s b_i K_i^n \cdot U^{ni} - \tau^2 \sum_{i,j=1}^s (b_i b_j - b_i a_{i,j} - b_j a_{j,i}) K_i^n \cdot K_j^n \\ &= \mathbf{0}. \end{aligned} \quad (2.34)$$

With noting the initial condition $Q^0 - (U^0)^2 = 0$, we obtain (2.32) from (2.34).

According to (2.30) and (2.31), we have

$$\begin{aligned} \mathcal{E}_h^{n+1} - \mathcal{E}_h^n &= \frac{\kappa}{2} \langle U^{n+1}, U^{n+1} \rangle_h + \frac{b}{2} \langle D_2 U^{n+1}, U^{n+1} \rangle_h + \frac{\beta}{3} \langle U^{n+1}, Q^{n+1} \rangle_h \\ &\quad - \frac{\kappa}{2} \langle U^n, U^n \rangle_h - \frac{b}{2} \langle D_2 U^n, U^n \rangle_h - \frac{\beta}{3} \langle U^n, Q^n \rangle_h \\ &= \frac{\tau \kappa}{2} \sum_{i=1}^s b_i \left(\langle U^n, K_i^n \rangle_h + \langle K_i^n, U^n \rangle_h \right) + \frac{\tau^2 \kappa}{2} \sum_{i,j=1}^s b_i b_j \langle K_i^n, K_j^n \rangle_h \\ &\quad + \frac{\tau b}{2} \sum_{i=1}^s b_i \left(\langle D_2 U^n, K_i^n \rangle_h + \langle D_2 K_i^n, U^n \rangle_h \right) + \frac{\tau^2 b}{2} \sum_{i,j=1}^s b_i b_j \langle D_2 K_i^n, K_j^n \rangle_h \end{aligned}$$

$$\begin{aligned}
& + \frac{\tau\beta}{3} \sum_{i=1}^s b_i \left(\langle U^n, L_i^n \rangle_h + \langle Q^n, K_i^n \rangle_h \right) + \frac{\tau^2\beta}{3} \sum_{i,j=1}^s b_i b_j \langle K_i^n, L_j^n \rangle_h \\
& = \tau \sum_{i=1}^s b_i \left(\kappa \langle U^{ni}, K_i^n \rangle_h + b \langle D_2 U^{ni}, K_i^n \rangle_h + \frac{\beta}{3} \langle U^{ni}, L_i^n \rangle_h + \frac{\beta}{3} \langle Q^{ni}, K_i^n \rangle_h \right) \\
& + \frac{\tau^2}{2} \kappa \sum_{i,j=1}^s (b_i b_j - b_i a_{ij} - b_j a_{ji}) \langle K_i^n, K_j^n \rangle_h \\
& + \frac{\tau^2}{2} \beta \sum_{i,j=1}^s (b_i b_j - b_i a_{ij} - b_j a_{ji}) \langle D_2 K_i^n, K_j^n \rangle_h \\
& + \frac{\tau^2}{3} \beta \sum_{i,j=1}^s (b_i b_j - b_i a_{ij} - b_j a_{ji}) \langle K_i^n, L_j^n \rangle_h.
\end{aligned}$$

With the condition (2.11) and the antisymmetry of \mathcal{J}_h , we have

$$\begin{aligned}
& \kappa \langle U^{ni}, K_i^n \rangle_h + b \langle D_2 U^{ni}, K_i^n \rangle_h + \frac{\beta}{3} \langle U^{ni}, L_i^n \rangle_h + \frac{\beta}{3} \langle Q^{ni}, K_i^n \rangle_h \\
& = \kappa \langle U^{ni}, K_i^n \rangle_h + b \langle D_2 U^{ni}, K_i^n \rangle_h + \frac{2\beta}{3} \langle (U^{ni})^2, K_i^n \rangle_h + \frac{\beta}{3} \langle Q^{ni}, K_i^n \rangle_h \\
& = \langle \kappa U^{ni} + b D_2 U^{ni} + \frac{2\beta}{3} (U^{ni})^2 + \frac{\beta}{3} Q^{ni}, K_i^n \rangle_h \\
& = \left\langle \kappa U^{ni} + b D_2 U^{ni} + \frac{\beta}{3} (2(U^{ni})^2 + Q^{ni}), \mathcal{J}_h \left(\kappa U^{ni} + b D_2 U^{ni} + \frac{\beta}{3} (2(U^{ni})^2 + Q^{ni}) \right) \right\rangle_h \\
& = 0,
\end{aligned}$$

which implies $\mathcal{E}_h^{n+1} = \mathcal{E}_h^n$. This completes the proof. \square

Remark 2.5. It follows from (2.32) and (2.33) that under the condition (2.11), the proposed **Scheme 2.2** can conserve the following discrete Hamiltonian energy

$$H_h^n = \frac{\kappa}{2} \|U^n\|^2 + \frac{b}{2} \langle D_2 U^n, U^n \rangle_h + \frac{\beta}{3} \langle U^n, (U^n)^2 \rangle_h, \quad n = 0, 1, 2, \dots, . \quad (2.35)$$

Theorem 2.8. For any RK method, **Scheme 2.2** conserves the following discrete mass

$$M_h^{n+1} = M_h^n, \quad M_h^n = \langle U^n, \mathbf{1} \rangle_h, \quad n = 0, 1, 2, \dots, . \quad (2.36)$$

Proof. It follows from the first equation of (2.31) that

$$M_h^{n+1} = M_h^n + \tau \sum_{i=1}^s b_i \langle K_i^n, \mathbf{1} \rangle_h. \quad (2.37)$$

Then, we can deduce from the first equation of (2.30) that

$$\begin{aligned}
\langle K_i^n, \mathbf{1} \rangle_h & = - \left\langle D_1 \left(\kappa U^{ni} + b D_2 U^{ni} + \frac{\beta}{3} (Q^{ni} + 2(U^{ni})^2) \right), \mathcal{A}_h^{-1} \mathbf{1} \right\rangle_h \\
& = - \left\langle D_1 \left(\kappa U^{ni} + b D_2 U^{ni} + \frac{\beta}{3} (Q^{ni} + 2(U^{ni})^2) \right), \mathbf{1} \right\rangle_h \\
& = 0.
\end{aligned}$$

This completes the proof. \square

Remark 2.6. Here, we introduce two notations, as follows:

- 4th-EPS: using 4th-Gauss collocation method to **Scheme 2.2**;
- 6th-EPS: using 6th-Gauss collocation method to **Scheme 2.2**.

3 An efficient implementation for the proposed schemes

In this section, motivated by [6, 32], we propose an efficient fixed pointed iteration solver for the nonlinear equations of the proposed schemes. For simplicity, we consider the 4th-MP scheme where the RK coefficient is given in Table 1. Note that the extensions to $s > 2$ are straightforward.

For given U^n , according to **Scheme 2.1**, the 4th-MP scheme is equivalent to

$$\mathcal{A}_h K_1^n = -[\kappa D_1 U^{n1} + b D_3 U^{n1} + \frac{p\beta}{p+1}((U^{n1})^{p-1} \cdot D_1 U^{n1} + D_1((U^{n1})^p))], \quad (3.1)$$

$$\mathcal{A}_h K_2^n = -[\kappa D_1 U^{n2} + b D_3 U^{n2} + \frac{p\beta}{p+1}((U^{n2})^{p-1} \cdot D_1 U^{n2} + D_1((U^{n2})^p))], \quad (3.2)$$

$$U^{n1} = U^n + \tau a_{11} K_1^n + \tau a_{12} K_2^n, \quad U^{n2} = U^n + \tau a_{21} K_1^n + \tau a_{22} K_2^n, \quad (3.3)$$

$$U^{n+1} = U^n + \tau b_1 K_1^n + \tau b_2 K_2^n, \quad (3.4)$$

It follows from (3.1)-(3.3) that

$$\mathcal{A}_h K_1^n = -[\tau \kappa a_{11} D_1 K_1^n + \tau \kappa a_{12} D_1 K_2^n + \tau b a_{11} D_3 K_1^n + \tau b a_{12} D_3 K_2^n + F_1], \quad (3.5)$$

$$\mathcal{A}_h K_2^n = -[\tau \kappa a_{21} D_1 K_1^n + \tau \kappa a_{22} D_1 K_2^n + \tau b a_{21} D_3 K_1^n + \tau b a_{22} D_3 K_2^n + F_2], \quad (3.6)$$

where

$$F_1 = \kappa D_1 U^n + b D_3 U^n + \frac{p\beta}{p+1}((U^{n1})^{p-1} \cdot D_1 U^{n1} + D_1((U^{n1})^p)),$$

$$F_2 = \kappa D_1 U^n + b D_3 U^n + \frac{p\beta}{p+1}((U^{n2})^{p-1} \cdot D_1 U^{n2} + D_1((U^{n2})^p)).$$

Using Remark 2.1, we can obtain from (3.5)-(3.6)

$$\mathcal{A}_h \mathbb{K}_1^n = -[\tau \kappa a_{11} \tilde{\Lambda} \mathbb{K}_1^n + \tau \kappa a_{12} \tilde{\Lambda} \mathbb{K}_2^n + \tau b a_{11} \tilde{\Lambda}^3 \mathbb{K}_1^n + \tau b a_{12} \tilde{\Lambda}^3 \mathbb{K}_2^n + \mathbb{F}_1], \quad (3.7)$$

$$\mathcal{A}_h \mathbb{K}_2^n = -[\tau \kappa a_{21} \tilde{\Lambda} \mathbb{K}_1^n + \tau \kappa a_{22} \tilde{\Lambda} \mathbb{K}_2^n + \tau b a_{21} \tilde{\Lambda}^3 \mathbb{K}_1^n + \tau b a_{22} \tilde{\Lambda}^3 \mathbb{K}_2^n + \mathbb{F}_2], \quad (3.8)$$

where $\mathcal{A}_h = I - \delta \Lambda^2 + \alpha \Lambda^4$ and $\mathbb{W} = \mathcal{F}_N W$.

For the nonlinear algebraic equations as above, we apply the following fixed point iteration strategy, for $l = 0, 1, 2, \dots, M$

$$\begin{bmatrix} \mathbb{A}_h + \tau \kappa a_{11} \tilde{\Lambda} + \tau b a_{11} \tilde{\Lambda}^3 & \tau \kappa a_{12} \tilde{\Lambda} + \tau b a_{12} \tilde{\Lambda}^3 \\ \tau \kappa a_{21} \tilde{\Lambda} + \tau b a_{21} \tilde{\Lambda}^3 & \mathbb{A}_h + \tau \kappa a_{22} \tilde{\Lambda} + \tau b a_{22} \tilde{\Lambda}^3 \end{bmatrix} \begin{bmatrix} \mathbb{K}_1^{n,l+1} \\ \mathbb{K}_2^{n,l+1} \end{bmatrix} = \begin{bmatrix} -\mathbb{F}_1^l \\ -\mathbb{F}_2^l \end{bmatrix},$$

which implies that

$$\begin{bmatrix} (\mathbb{A}_h)_j + \tau \kappa a_{11} \tilde{\Lambda}_j + \tau b a_{11} \tilde{\Lambda}_j^3 & \tau \kappa a_{12} \tilde{\Lambda}_j + \tau b a_{12} \tilde{\Lambda}_j^3 \\ \tau \kappa a_{21} \tilde{\Lambda}_j + \tau b a_{21} \tilde{\Lambda}_j^3 & (\mathbb{A}_h)_j + \tau \kappa a_{22} \tilde{\Lambda}_j + \tau b a_{22} \tilde{\Lambda}_j^3 \end{bmatrix} \begin{bmatrix} (\mathbb{K}_1^{n,l+1})_j \\ (\mathbb{K}_2^{n,l+1})_j \end{bmatrix} = \begin{bmatrix} -(\mathbb{F}_1^l)_j \\ -(\mathbb{F}_2^l)_j \end{bmatrix},$$

where $j = 0, 1, \dots, N-1$.

Solving the above equations, we obtain $\mathbb{K}_1^{n,l+1}$ and $\mathbb{K}_2^{n,l+1}$. Then $K_1^{n,l+1}$ and $K_2^{n,l+1}$ are given by $K_1^{n,l+1} = \mathcal{F}_N^H \mathbb{K}_1^{n,l+1}$ and $K_2^{n,l+1} = \mathcal{F}_N^H \mathbb{K}_2^{n,l+1}$, respectively. In our computations, we take the iterative initial value $K_1^{n,0} = U^n$ and $K_2^{n,0} = U^n$. The iteration terminates when the number of maximum iterative step $M = 30$ is reached or the infinity norm of the error between two adjacent iterative steps is less than 10^{-14} , that is

$$\max_{l \leq i \leq 2} \{ \|K_i^{n,l+1} - K_i^{n,l}\|_{\infty, h} \} < 10^{-14}.$$

Finally, we have $U^{n+1} = U^n + \tau b_1 K_1^{n,M} + \tau b_2 K_2^{n,M}$.

Remark 3.1. Similarly, the efficient iteration solver for the resulting nonlinear equations of the 4th-EP scheme (see **Scheme 2.2**) is given by, as follows:

$$\begin{bmatrix} I - \tau\kappa a_{11}J_h - \tau b a_{11}J_h\Lambda^2 & -\tau\kappa a_{12}J_h - \tau b a_{12}J_h\Lambda^2 \\ -\tau\kappa a_{21}J_h - \tau b a_{21}J_h\Lambda^2 & I - \tau\kappa a_{22}J_h - \tau b a_{22}J_h\Lambda^2 \end{bmatrix} \begin{bmatrix} \mathbb{K}_1^{n,l+1} \\ \mathbb{K}_2^{n,l+1} \end{bmatrix} = \begin{bmatrix} \mathbb{F}_1^l \\ \mathbb{F}_2^l \end{bmatrix},$$

where

$$\begin{aligned} F_1 &= \mathcal{J}_h \left(\kappa U^n + b D_2 U^n + \frac{\beta}{3} (Q^{n1} + 2(U^{n1})^2) \right), \\ F_2 &= \mathcal{J}_h \left(\kappa U^n + b D_2 U^n + \frac{\beta}{3} (Q^{n2} + 2(U^{n2})^2) \right), \\ U^{ni} &= U^n + \tau a_{i1} K_1^n + \tau a_{i2} K_2^n, \quad J_h = -(I - \delta\Lambda^2 + \alpha\Lambda^4)^{-1} \tilde{\Lambda}, \\ Q^{ni} &= (U^n)^2 + \tau \sum_{j=1}^s a_{ij} L_j^n, \quad L_i^n = 2U^{ni} \cdot K_i^n, \quad i = 1, 2, \end{aligned}$$

In particular, the iteration equations as stated above can be rewritten into the following subsystems

$$\begin{bmatrix} 1 - \tau\kappa a_{11}(J_h)_j - \tau b a_{11}(J_h)_j \Lambda_j^2 & -\tau\kappa a_{12}(J_h)_j - \tau b a_{12}(J_h)_j \Lambda_j^2 \\ -\tau\kappa a_{21}(J_h)_j - \tau b a_{21}(J_h)_j \Lambda_j^2 & 1 - \tau\kappa a_{22}(J_h)_j - \tau b a_{22}(J_h)_j \Lambda_j^2 \end{bmatrix} \begin{bmatrix} (\mathbb{K}_1^{n,l+1})_j \\ (\mathbb{K}_2^{n,l+1})_j \end{bmatrix} = \begin{bmatrix} (\mathbb{F}_1^l)_j \\ (\mathbb{F}_2^l)_j \end{bmatrix},$$

where $j = 0, 1, 2, \dots, N-1$. Then, by the similar procedure as the 4th-MP scheme, we have U^{n+1} .

4 Numerical results

In this section, we devote to the numerical performances in the accuracy and invariants-preservation of the proposed schemes for the equation (1.1). For brevity, in the rest of this paper, 4th-MPS, 4th-EPS, 6th-MPS and 6th-EPS are only used for demonstration purposes. In order to quantify the numerical solution, we introduce the l^2 - and l^∞ -norm error functions, respectively,

$$e_\infty(t_n) = \|u(\cdot, t_n) - u^n\|_{l^\infty}, \quad e_2(t_n) = \|u(\cdot, t_n) - u^n\|_{l^2}.$$

Furthermore, we also investigate the residuals on the mass, momentum and Hamiltonian energy, defined respectively, as

$$Errorr_1^n = |M_h^n - M_h^0|, \quad Errorr_2^n = |I_h^n - I_h^0|, \quad Errorr_3^n = |H_h^n - H_h^0|.$$

All simulations are performed on a Win10 machine with Intel Core i7 and 32GB using MATLAB R2015b.

4.1 Rosenau-RLW equation

As the parameters $\kappa = \delta = \alpha = \beta = 1$ and $b = 0$, the equation (1.1) reduces to the generalized Rosenau-RLW equation, which has an exact solution [4, 20]

$$u(x, t) = A \operatorname{sech}^{\frac{4}{p-1}}(B(x - Ct - x_0)), \quad (4.1)$$

where

$$A = \exp\left(\frac{\ln \frac{(p+3)(3p+1)(p+1)}{2(p^2+3)(p^2+4p+7)}}{p-1}\right), \quad B = \frac{p-1}{\sqrt{4p^2+8p+20}}, \quad C = \frac{p^4+4p^3+14p^2+20p+25}{p^4+4p^3+10p^2+12p+21},$$

and x_0 represents the initial phase of the soliton and the periodic boundary condition is considered.

We first verify the convergence order in time for the proposed schemes. Let us set the computational domain $\Omega = [-200, 200]$ and we take the initial value

$$u(x, 0) = A \operatorname{sech}^{\frac{4}{p-1}}(B(x - x_0)), \quad x \in \Omega,$$

where the initial phase $x_0 = 0$.

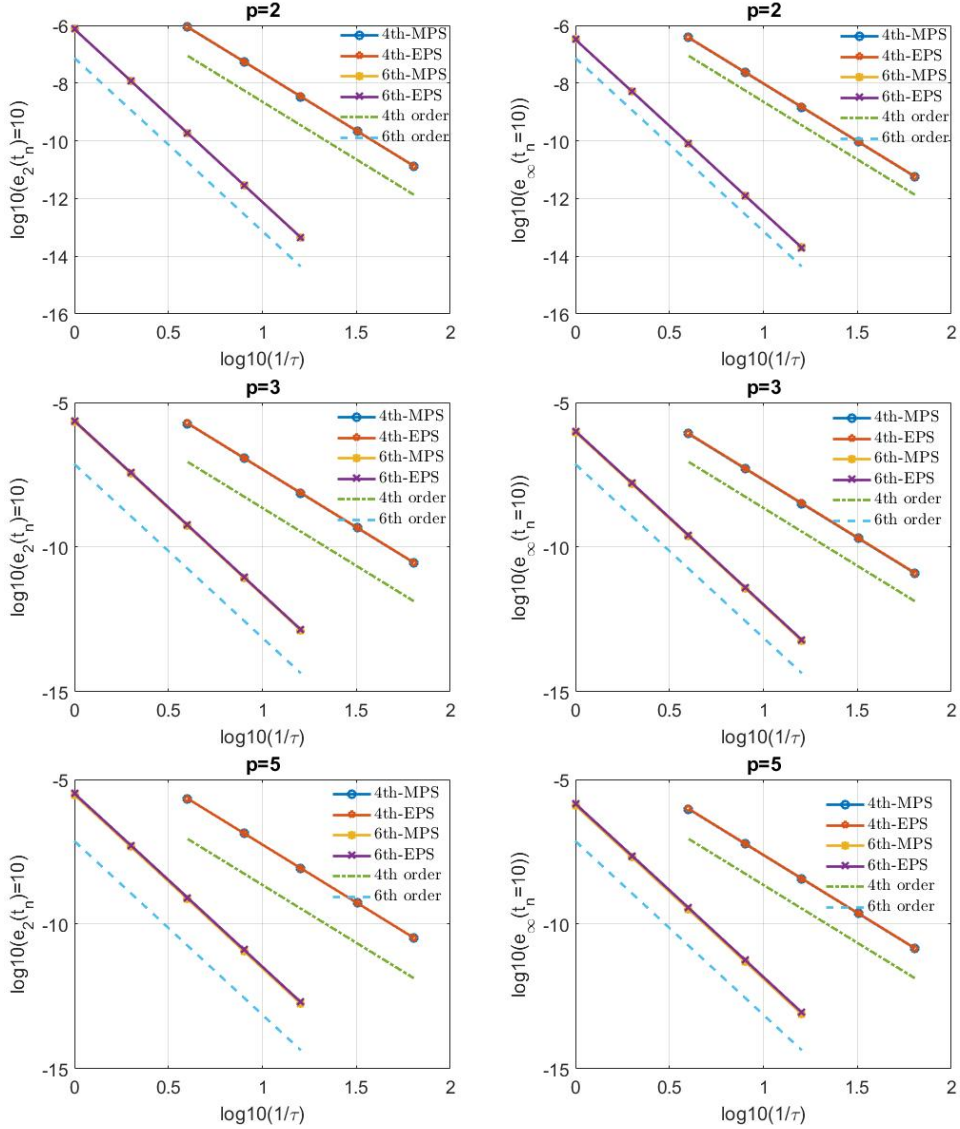


Fig. 1: The l^2 and l^∞ -norm errors vs. the time step size produced by the proposed 4th-MPS, 4th-EPS, 6th-MPS and 6th-EPS for the Rosenau-RLW equation with the parameters $p = 2$ (up), $p = 3$ (middle) and $p = 5$ (down), respectively.

The temporal convergence tests are investigated by fixing the Fourier node 2048. We compute the numerical solutions at $t = 10$ using 4th-MPS and 4th-EPS with various time step sizes $\tau = 2^{-k}$, $k = 2, 3, 4, 5, 6$ as well as 6th-MPS and 6th-EPS with various time step sizes $\tau = 2^{-k}$, $k = 0, 1, 2, 3, 4$, respectively. The relation between the l^2 and l^∞ -norm errors and the time step size is summarized in Figure 1, where the up picture

corresponds to the parameter $p = 2$, the middle one corresponds to the parameter $p = 3$ and the down one is for the parameter $p = 5$. The fourth-order temporal accuracy for 4th-MPS and 4th-EPS and the sixth-order for 6th-MPS and 6th-EPS are observed, respectively, for different parameters p as desired.

Then, we choose the initial value, as follows:

$$u(x, 0) = \exp(-0.05(x - 40)^2), \quad x \in \Omega, \quad (4.2)$$

where the computational domain $\Omega = [-50, 250]$ with the periodic boundary condition. We take the uniform spatial and time mesh $\tau = h = 0.1$, and compute the profile of u at $T = 100$ by choosing different parameters p as well as the residuals on the discrete mass, momentum and Hamiltonian energy by using 4th-MPS, 4th-EPS, 6th-MPS and 6th-EPS, respectively. Figure 2 shows the profile of u provided by 4th-MPS at $t = 100$, where the left picture corresponds to the parameter $p = 2$, the middle one corresponds to the parameter $p = 3$ and the right one is for the parameter $p = 5$. The influence of the parameter p on the dispersion wave propagation is observed as shown in [7]. We should note that the profiles of u at $t = 100$ computed using other schemes are similar to Figure 2, thus for brevity, we omit them. Figure 3 shows the evolutions of the residuals on the discrete mass, momentum and Hamiltonian energy of numerical solutions computed by 4th-MPS, 4th-EPS, 6th-MPS and 6th-EPS, respectively. We can draw the following observations: (1) for the parameter $p = 2$, all of proposed schemes preserve the discrete mass exactly, while the proposed momentum-preserving schemes cannot conserve the discrete mass for the parameters $p = 3$ and $p = 5$; (2) 4th-MPS and 6th-MPS can preserve discrete momentum up to the machine precision; (3) 4th-EPS and 6th-EPS conserve the discrete both mass and Hamiltonian energy for all parameters p .

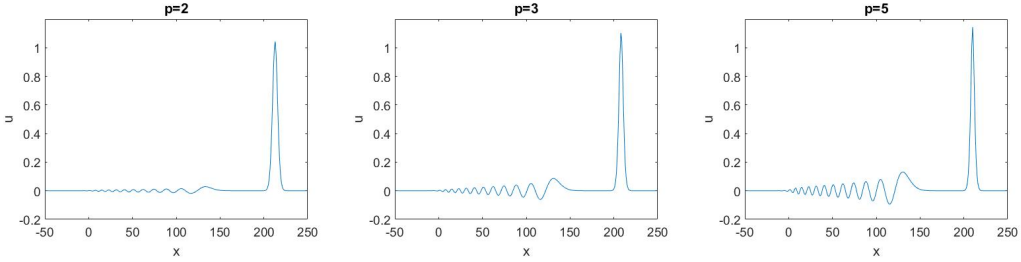
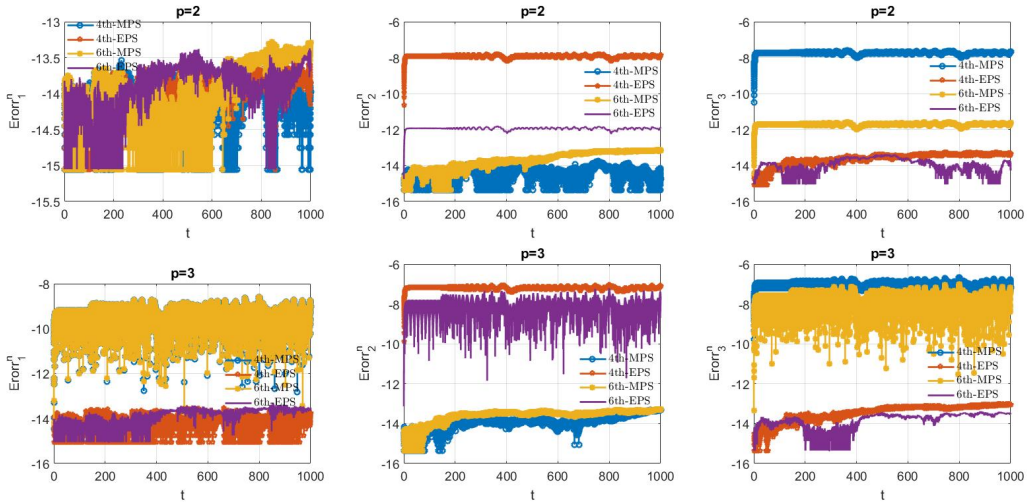


Fig. 2: The profile of u provided by 4th-MPS with different parameters $p = 2$ (left), $p = 3$ (middle) and $p = 5$ (right) at $t = 100$, where the uniform spatial and time mesh is chosen by $\tau = h = 0.1$ for the Rosenau-RLW equation.



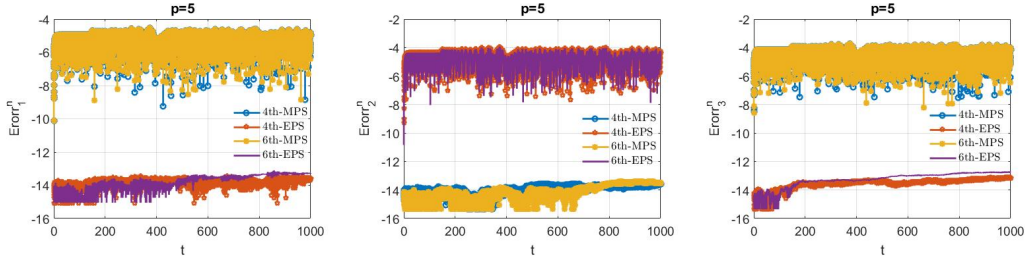


Fig. 3: The residuals on the discrete mass, momentum and Hamiltonian energy from $t = 0$ to $t = 1000$ produced by the proposed 4th-MPS, 4th-EPS, 6th-MPS and 6th-EPS for the Rosenau-RLW equation with the parameters $p = 2$ (up), $p = 3$ (middle) and $p = 5$ (down).

4.2 Rosenau-KdW equation

As the parameters $\kappa = b = \alpha = 1$ and $\delta = 0$, the equation (1.1) reduces to the generalized Rosenau-KdV equation[33]. For simplicity, we also consider the parameters $p = 2$, $p = 3$ and $p = 5$, respectively, where the exact solution can be given by

Case I: As $\beta = \frac{1}{2}$ and $p = 2$, the Rosenau-KdV equation has an exact solution [13]

$$u(x, t) = k_{11} \operatorname{sech}^4(k_{12}(x - k_{13}t)). \quad (4.3)$$

where $k_{11} = -\frac{35}{24} + \frac{35}{312}\sqrt{313}$, $k_{12} = \frac{1}{24}\sqrt{-26 + 2\sqrt{313}}$, $k_{13} = \frac{1}{2} + \frac{\sqrt{313}}{26}$.

Case II: If $\beta = 1$ and $p = 3$, the Rosenau-KdV equation admits an exact solution [22]

$$u(x, t) = k_{21} \operatorname{sech}^2(k_{22}(x - k_{23}t)), \quad (4.4)$$

where $k_{21} = \frac{1}{4}\sqrt{-15 + 3\sqrt{41}}$, $k_{22} = \frac{1}{4}\sqrt{\frac{-5 + \sqrt{41}}{2}}$, $k_{23} = \frac{1}{10}(5 + \sqrt{41})$.

Case III: When $\beta = 1$ and $p = 5$, the exact solution of the Rosenau-KdV equation is given by [33]

$$u(x, t) = k_{31} \operatorname{sech}^2(k_{32}(x - k_{33}t)), \quad (4.5)$$

where $k_{31} = \sqrt[4]{\frac{4}{15}(-5 + \sqrt{34})}$, $k_{32} = \frac{1}{3}\sqrt{-5 + \sqrt{34}}$, $k_{33} = \frac{1}{10}(5 + \sqrt{34})$.

First of all, we verify the convergence order in time for the selected four structure-preserving schemes. Let us set the computational domain $\Omega = [-200, 200]$ and we take the initial value as the exact solution at $t = 0$ for the parameters $p = 2$, $p = 3$ and $p = 5$, respectively. The temporal convergence tests are conducted by fixing the Fourier node 2048. Figure 4 shows the l^2 and l^∞ -norm errors with various time step sizes at $t = 10$, where we take time step sizes $\tau = 2^{-k}$, $k = 2, 3, 4, 5, 6$ for 4th-MPS and 4th-EPS, while for 6th-MPS and 6th-EPS, we choose time step sizes $\tau = 2^{-k}$, $k = 0, 1, 2, 3, 4$. It is clear to see that 4th-MPS and 4th-EPS are fourth-order temporal accuracy, and 6th-MPS and 6th-EPS can achieve sixth-order accurate in time.

Then, we set the computational domain $\Omega = [-100, 100]$ and take the uniform spatial mesh $h = \frac{200}{512}$ and time mesh $\tau = 0.1$, respectively. Figure 5 shows the residuals on the discrete mass, momentum and Hamiltonian energy computed by using 4th-MPS, 4th-EPS, 6th-MPS and 6th-EPS, respectively, which is similar to Figure 3. We should note that the residuals on the discrete mass provided by 4th-MPS and 6th-MPS is also up to the machine precision because of the small spatial mesh.

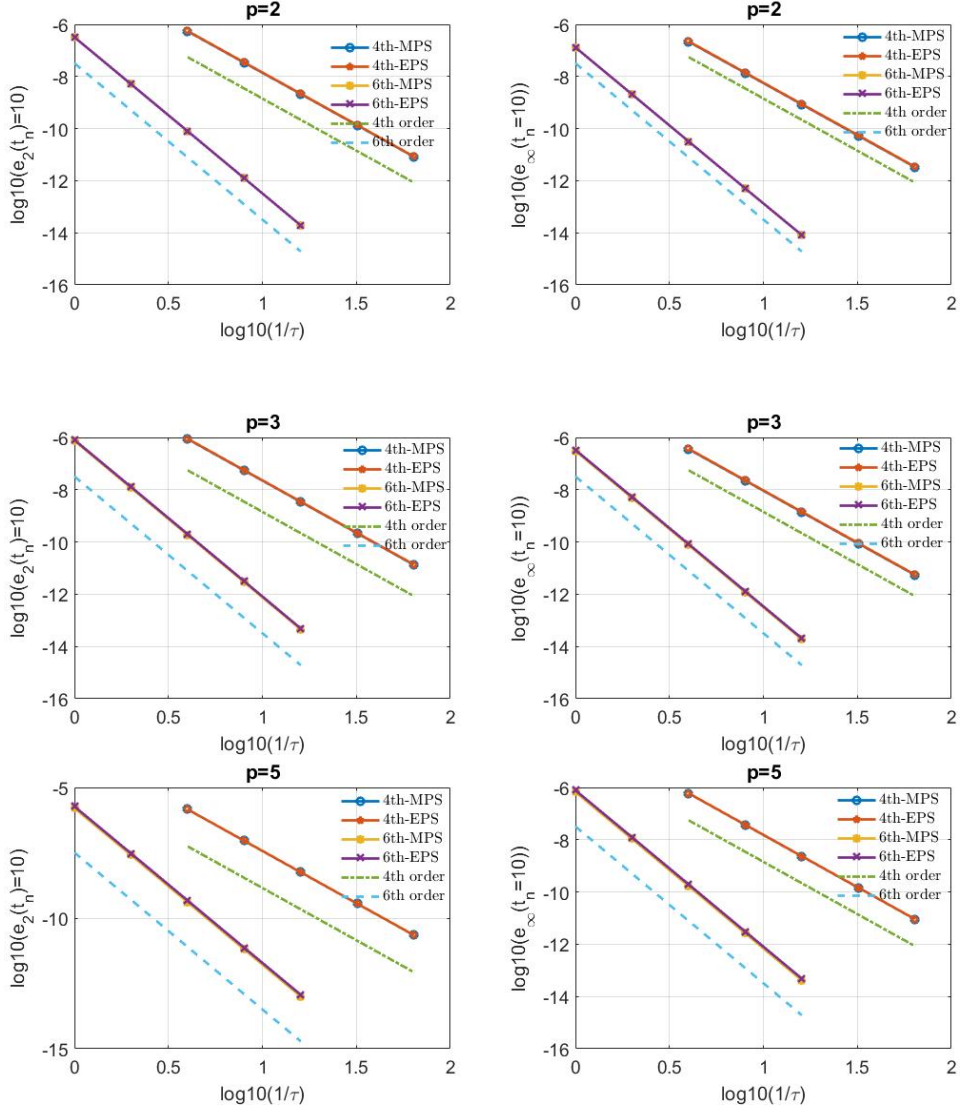
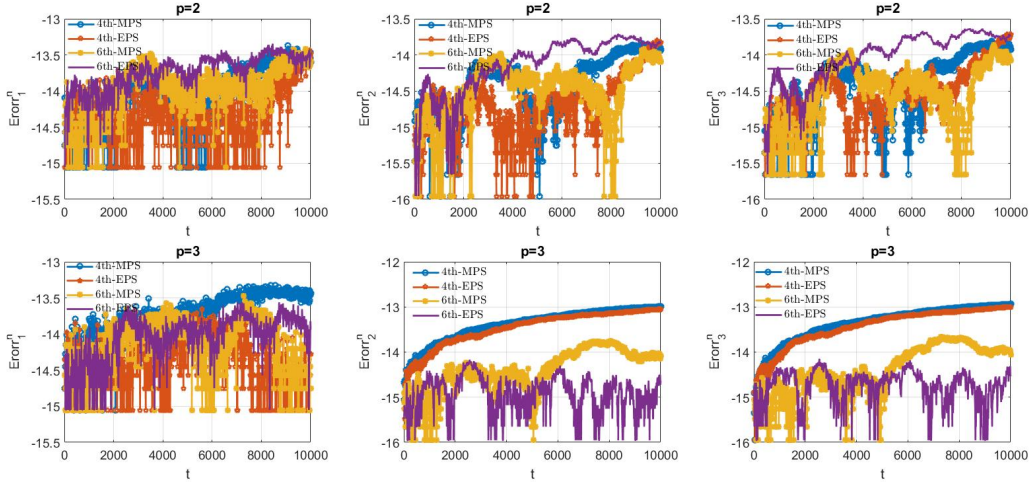


Fig. 4: The l^2 and l^∞ -norm errors vs. the time step size produced by the proposed 4th-MPS, 4th-EPS, 6th-MPS and 6th-EPS for the Rosenau-KdV equation with the parameters $p = 2$ (up), $p = 3$ (middle) and $p = 5$ (down), respectively.



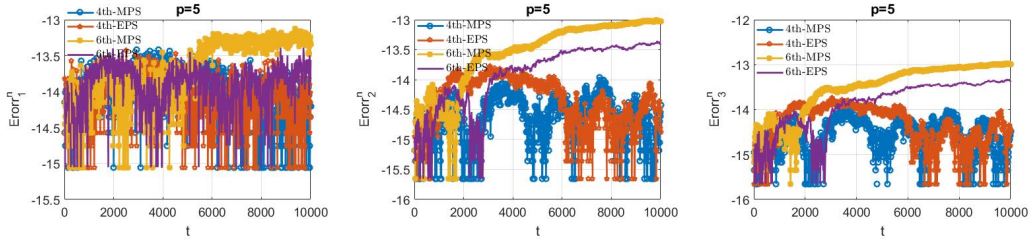


Fig. 5: The residuals on the mass, momentum and Hamiltonian energy from $t = 0$ to $t = 10000$ produced by the proposed 4th-MPS, 4th-EPS, 6th-MPS and 6th-EPS for the Rosenau-RdV equation with the parameters $p = 2$ (up), $p = 3$ (middle) and $p = 5$ (down).

4.3 Some comparisons

In the following numerical experiments, we compare the proposed structure-preserving schemes with the linearized Crank-Nicolson momentum-preserving scheme (LCN-MPS) [15] and fourth-order energy-preserving schemes (i.e., YC-EPS and SC-EPS) [3] by focusing on the numerical errors in time and the computational efficiency.

Let us still consider the Rosenau-KdW equation as above. For the sake of simplicity, we only consider the parameter $p = 2$ (see Case I in Section 4.2). We set the computational domain $\Omega = [-100, 100]$ and the uniform spatial mesh $h = \frac{200}{1024}$. Table 2 shows the numerical errors and convergence order in time for the different schemes with various time steps at $t = 1$. It is clear to observe that (i) LCN-MPS is second-order accurate in time and its numerical errors are largest; (ii) 4th-MPS, 4th-EPS, YC-EPS and SC-EPS are all fourth-order accurate in time, and the numerical error provided by SC-EPS is smallest, while the ones provided by YC-EPS are much larger than other fourth-order schemes.

Finally, we investigate the global l^2 - and l^∞ - errors of u versus the CPU time using the five selected structure-preserving schemes with the Fourier node 2^{13} and various time steps at $t = 30$. The results are summarized in Figure 6. For a given global error, we observe that (i) the cost of the LCN-MP scheme is the most expensive because of the low-order accuracy in time; (ii) the cost of 4th-EPS is the cheapest; (iii) the costs of SC-EPS are much cheaper than the ones provided by the 4th-MP scheme, and the costs of 4th-MPS are much cheaper than the ones provided by the YC-EP scheme.

5 Conclusion

In this paper, we propose two class of high-order structure-preserving schemes for the generalized Rosenau-type equation (1.1). One of the schemes can conserve the discrete momentum conservation law, which is based on the use of the symplectic RK method in time and the standard Fourier pseudo-spectral method in space, respectively. Another one conserves the discrete Hamiltonian energy and mass, where the main idea is based on the combination of the QAV approach with the the symplectic RK method in time, together with the standard Fourier pseudo-spectral method in space. Extensive numerical tests and comparisons are also addressed to verify the performance of the proposed schemes. However, we should note that the proposed schemes involves solving a fully nonlinear equations at every time step. Therefore, it is interesting to develop high-order linearly implicit structure-preserving schemes, in which a linear system is to be solved at every time step, in our future works.

Table. 2: Numerical errors and convergence order for the different schemes with various time steps at $t = 1$.

Scheme	τ	$e_2(t_n = 1)$	order	$e_\infty(t_n = 1)$	order
4th-EPS	$\frac{1}{10}$	1.585e-09	-	6.292e-10	-
	$\frac{1}{20}$	9.905e-11	4.000	3.933e-11	4.000
	$\frac{1}{40}$	6.191e-12	4.000	2.458e-12	4.000
	$\frac{1}{80}$	3.867e-13	4.001	1.540e-13	3.997
	$\frac{1}{10}$	1.518e-09	-	5.984e-10	-
4th-MPS	$\frac{1}{20}$	9.490e-11	4.000	3.740e-11	4.000
	$\frac{1}{40}$	5.932e-12	4.000	2.338e-12	4.000
	$\frac{1}{80}$	3.706e-13	4.000	1.462e-13	3.999
	$\frac{1}{10}$	7.299e-05	-	2.800e-05	-
	LCN-MPS[15]	$\frac{1}{20}$	1.813e-05	2.009	6.950e-06
$\frac{1}{40}$		4.518e-06	2.005	1.731e-06	2.006
$\frac{1}{80}$		1.128e-06	2.002	4.319e-07	2.003
$\frac{1}{10}$		8.024e-08	-	3.400e-08	-
YC-EPS [3]		$\frac{1}{20}$	5.024e-09	3.997	2.129e-09
	$\frac{1}{40}$	3.142e-10	3.999	1.331e-10	3.999
	$\frac{1}{80}$	1.964e-11	4.000	8.326e-12	4.000
	$\frac{1}{10}$	1.081e-09	-	4.355e-10	-
	SC-EPS [3]	$\frac{1}{20}$	6.761e-11	4.000	2.723e-11
$\frac{1}{40}$		4.229e-12	3.999	1.708e-12	3.995
$\frac{1}{80}$		2.896e-13	3.868	1.186e-13	3.848

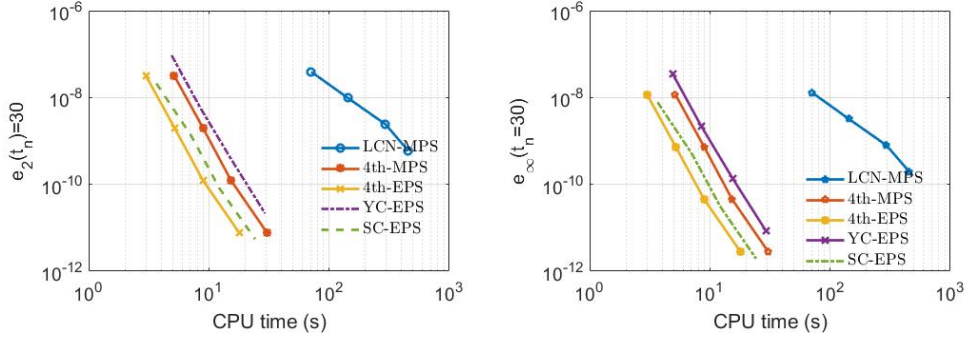


Fig. 6: The l^2 and l^∞ -norm errors vs. the CPU time produced by LCN-MPS, 4th-MPS, 4th-EPS, YC-EPS and SC-EPS for the Rosenau-KdV equation.

Acknowledgment

The work is supported by the National Natural Science Foundation of China (Grant Nos. 11901513, 11971481), and the Yunnan Fundamental Research Projects (Grant No. 202101AT070208), and the Natural Science Foundation of Hunan (Grant Nos. 2021JJ40655, 2021JJ20053).

References

- [1] M. Ahmat and J. Qiu. SSP IMEX Runge-Kutta WENO scheme for generalized Rosenau-KdV-RLW equation. *J. Math. Study.*, 55:1–21, 2022.
- [2] N. Atouani and K. Omrani. A new conservative high-order accurate difference scheme for the Rosenau equation. *Appl. Anal.*, 94:2435–2455, 2015.
- [3] J. Cai, H. Liang, and C. Zhang. Efficient high-order structure-preserving methods for the generalized Rosenau-type equation with power law nonlinearity. *Commun. Nonlinear Sci. Numer. Simulat.*, 59:122–131, 2018.
- [4] W. Cai, Y. Sun, and Y. Wang. Variational discretizations for the generalized Rosenau-type equations. *Appl. Math. Comput.*, 271:860–873, 2015.
- [5] S. K. Chung. Finite difference approximate solutions for the Rosenau equation. *Appl. Anal.*, 69:149–156, 1998.
- [6] J. Cui, Y. Wang, and C. Jiang. Arbitrarily high-order structure-preserving schemes for the Gross-Pitaevskii equation with angular momentum rotation. *Comput. Phys. Commun.*, 261:107767, 2021.
- [7] Y. I. Dimitrienko, S. Li, and Y. Niu. Study on the dynamics of a nonlinear dispersion model in both 1D and 2D based on the fourth-order compact conservative difference scheme. *Math. Comput. Simulat.*, 182:661–689, 2021.
- [8] Y. Gong, J. Cai, and Y. Wang. Multi-symplectic Fourier pseudospectral method for the Kawahara equation. *Commun. Comput. Phys.*, 16:35–55, 2014.
- [9] Y. Gong, Q. Hong, C. Wang, and Y. Wang. Quadratic auxiliary variable Runge-Kutta methods for the Camassa-Holm equation. *Preprint*.
- [10] Y. Gong, J. Zhao, and Q. Wang. Arbitrarily high-order linear energy stable schemes for gradient flow models. *J. Comput. Phys.*, 419:109610, 2020.
- [11] E. Hairer, C. Lubich, and G. Wanner. *Geometric Numerical Integration: Structure-Preserving Algorithms for Ordinary Differential Equations*. Springer-Verlag, Berlin, 2nd edition, 2006.
- [12] D. He. Exact solitary solution and a three-level linearly implicit conservative finite difference method for the generalized Rosenau-Kawahara-RLW equation with generalized Novikov type perturbation. *Nonlinear Dyn.*, 85:479–498, 2016.
- [13] J. Hu, Y. Xu, and B. Hu. Conservative linear difference scheme for Rosenau-KdV equation. *Adv. Math. Phys.*, pages 1–7, 2013.
- [14] C. Jiang, W. Cai, Y. Wang, and H. Li. A novel sixth order energy-conserved method for three-dimensional time-domain Maxwell’s equations. *arXiv:1705.08125*, 2017.
- [15] C. Jiang, J. Cui, W. Cai, and Y. Wang. A novel linearized and momentum-preserving fourier pseudo-spectral scheme for the Rosenau-Korteweg de Vries equation. *arXiv:1901.04667*, 2019.
- [16] C. Jiang, J. Cui, X. Qian, and S. Song. High-order linearly implicit structure-preserving exponential integrators for the nonlinear Schrödinger equation. *J. Sci. Comput.*, 90, 2022, doi.org/10.1007/s10915-021-01739-x.

- [17] C. Jiang, Y. Wang, and Y. Gong. Arbitrarily high-order energy-preserving schemes for the Camassa-Holm equation. *Appl. Numer. Math.*, 151:85–97, 2020.
- [18] S. Li. Numerical analysis for fourth-order compact conservative difference scheme to solve the 3D Rosenau-RLW equation. *Comput. Math. Appl.*, 72:2388–2407, 2016.
- [19] K. Omrani, F. Abidi, T. Achouri, and N. Khiari. A new conservative finite difference scheme for the Rosenau equation. *Appl. Math. Comput.*, 201:35–43, 2008.
- [20] X. Pan and L. Zhang. On the convergence of a conservative numerical scheme for the usual Rosenau-RLW equation. *Appl. Mathe. Model.*, 36:3371–3378, 2012.
- [21] G. R. W. Quispel and D. I. McLaren. A new class of energy-preserving numerical integration methods. *J. Phys. A: Math. Theor.*, 41:045206, 2008.
- [22] P. Razborova, L. Moraru, and A. Biswas. Perturbation of dispersive shallow water waves with Rosenau-KdV-RLW equation and power law nonlinearity. *Rom. J. Phys.*, 59:658–676, 2014.
- [23] P. Rosenau. Dynamics of dense discrete systems: high order effects. *Progr. Theor. Phys.*, 79:1028–1042, 1988.
- [24] J. M. Sanz-Serna. Runge-Kutta schemes for Hamiltonian systems. *BIT*, 28:877–883, 1988.
- [25] J. M. Sanz-Serna and M. Calvo. *Numerical Hamiltonian Problems*. Chapman & Hall, London, 1994.
- [26] J. Shen and T. Tang. *Spectral and High-Order Methods with Applications*. Science Press, Beijing, 2006.
- [27] H. Wang, S. Li, and J. Wang. A conservative weighted finite difference scheme for the generalized Rosenau-RLW equation. *Comput. Math. Appl.*, 36:63–78, 2017.
- [28] J. Wang and Q. Zeng. A fourth-order compact and conservative difference scheme for the generalized Rosenau-Korteweg de Vries equation in two dimensions. *J. Comput. Math.*, 37:541–555, 2019.
- [29] X. Wang and W. Dai. A new implicit energy conservative difference scheme with fourth-order accuracy for the generalized Rosenau-Kawahara-RLW equation. *Comput. Appl. Math.*, 37:6560–6581, 2018.
- [30] X. Wang, W. Dai, and Y. Yan. Numerical analysis of a new conservative scheme for the 2D generalized Rosenau-RLW equation. *Appl. Anal.*, 100:2564–2580, 2021.
- [31] B. Wongsaijai, P. Charoensawan, T. Chaobankoh, and K. Pochinapan. Advance in compact structure-preserving manner to the Rosenau-Kawahara model of shallow-water wave. *Math. Meth. Appl. Sci.*, 44:7048–7064, 2021.
- [32] G. Zhang and C. Jiang. Arbitrary high-order structure-preserving methods for the quantum Zakharov system. *arXiv:2202.13052*, 2022.
- [33] M. Zheng and J. Zhou. An average linear difference scheme for the generalized Rosenau-KdV equation. *J. Appl. Math.*, pages 1–9, 2014.